Comparative Polymerization in the Gas Phase and in Clusters. 1. Covalent Dimer Formation and Entropy Barriers to Polymerization in Isobutene

Michael Meot-Ner (Mautner),*,†,‡ L. Wayne Sieck,† M. Samy El-Shall,*,‡ and George M. Daly‡

Contribution from the Chemical Kinetics and Thermodynamics Division, National Institute of Standards and Technology, Gaithersburg, Maryland 20899, and the Department of Chemistry, Virginia Commonwealth University, Richmond, Virginia 23284-2006

Received March 15, 1995[⊗]

Abstract: This work presents kinetic and thermochemical data for ionic polymerization in the gas phase, and the following paper bridges toward the condensed phase by cluster measurements. Gas-phase measurements by pulsed high-pressure mass spectrometry involving reactions in the radical and protonated ion branches in isobutene lead to the following observations. (1) $i\text{-}C_4H_8^{\bullet+} + i\text{-}C_4H_8 \rightarrow t\text{-}C_4H_9^+$ is fast ($k = 0.5 \pm 0.1 \times 10^{-9}$ cm^3 s^{-1}) from 250 to 625 K, but the competing condensation to form $C_8H_{16}^{\bullet+}$ decreases with increasing temperature ($k_{250} = 1.4 \times 10^{-9}$ cm^3 s^{-1}, $k_{497} = 0.2 \times 10^{-9}$ cm^3 s^{-1}). The distinct behavior suggests two collision types, leading to direct reaction or complex formation. (2) The product $C_8H_{16}^{\bullet+}$ is identified as a covalent adduct with a dissociation energy >132 kJ/mol (32 kcal/mol), and bracketing experiments confirm it as an octene ion corresponding to an IP of 8.55 ± 0.15 eV. (3) The adduct undergoes H_2 transfer to $i\text{-}C_4H_8$, and the rate coefficient has a large negative temperature coefficient of $T^{-4.3}$. The product is unreactive toward further polymerization. (4) In the protonated (carbonium ion) branch, consecutive association reactions have decreasing rate coefficients. (5) The first step in the protonated branch, forming $C_8H_{17}^+$, is reversible and the thermochemistry [$\Delta H° = -95.8$ kJ/mol (−22.9 kcal/mol), $\Delta S° = -136.8$ J/(mol K) (−32.7 cal/(mol K))] is consistent with the formation of a tertiary carbonium ion. The thermochemistry of the second step exhibits an unusually large negative entropy change [$\Delta H° = -101.3$ kJ/mol (−24.2 kcal/mol), $\Delta S° = -203.7$ J/(mol K) (−48.7 cal/(mol K))] and a rate coefficient with a very large negative temperature coefficient (T^{-12} to T^{-16}). Both observations suggest a highly constrained product, whose formation constitutes an entropy barrier to the polymerization sequence. (6) A novel H_2 transfer reaction, from the carbonium ion $C_8H_{17}^+$ to $i\text{-}C_4H_8$, is observed, and the rate coefficient has a negative temperature coefficient. The results suggest that ionic polymerization reactions that involve steric entropy barriers will be slow under flame conditions but fast at low interstellar temperatures. The temperature coefficients explain the need for using low temperatures in the industrial polymerization of isobutene.

Introduction

Ionic polymerization plays important roles in condensed phase processes, as well as in the gas phase in flames and in interstellar synthesis. For understanding such processes, quantitative kinetic and thermochemical data on the individual steps are needed. Although it is impractical to observe individual steps in the condensed phase, the isolated steps can be studied in the gas phase. Even if gas-phase data are obtained, however, it may be questioned if they can be applied meaningfully to the condensed phase. This question can be addressed by reactions in clusters, which present an environment intermediate between the gas and condensed phases. Indeed, we and others recently demonstrated ionic polymerization in clusters,[1−4] which showed similarities to gas phase ion−molecule reactions. The comparative gas-phase and cluster behavior will be discussed in the following paper.

Gas-phase polymerization involving carbocations has been studied in several systems,[5−12] including the present system of interest, $i\text{-}C_4H_8$.[5−8] Those studies involve rate coefficients and product distributions at 300 K. A general observation is that the first step occurs near the collision rate, but after one or two further steps, the rate coefficients become slower by orders of magnitude.

The available kinetic data provide little insight into the rate controlling factors, for example, on the relative rates of consecutive steps, or the effects of the environment such as partial solvation, or the variation with temperature. The latter is important as application to high-temperature flames and low-temperature interstellar processes, both of which produce large hydrocarbons through ionic polymerization. Temperature effects are also important for optimizing industrial processes. Studying temperature effects in polymerization is important since some ion−molecule reactions have large positive or negative temperature coefficients.[13−15]

Experimental Section

The experiments were performed using the NIST pulsed high-pressure mass spectrometer.[16] For experiments involving radical ions, the carrier gas was N_2 at ion source pressures of 4−10 mbar, with

† National Institute of Standards and Technology.
‡ Virginia Commonwealth University.
⊗ Abstract published in *Advance ACS Abstracts*, July 1, 1995.

(1) El-Shall, M. S.; Marks, C. *J. Phys. Chem.* **1991**, *95*, 4932.
(2) El-Shall, M. S.; Schriver, K. E. *J. Chem. Phys.* **1991**, *95*, 3001.
(3) Daly, G. M.; El-Shall, M. S. *Z. Phys. D* **1993**, *26*, S 186.
(4) Coolbaugh, M. T.; Vaidyanathan, G.; Pelfer, W. R.; Garvey, J. F. *J. Phys. Chem.* **1991**, *95*, 8337.
(5) Aquilanti, V.; Galli, A.; Giordini-Guidoni, A.; Volpi, G. G. *Trans. Faraday Soc.* **1967**, *63*, 926.
(6) Sieck, L. W.; Searles, S. K.; Ausloos, P. *J. Am. Chem. Soc.* **1969**, *91*, 7627.
(7) Henis, J. M. S. *J. Chem. Phys.* **1970**, *52*, 282.
(8) Sieck, L. W.; Ausloos, P. *J. Chem. Phys.* **1972**, *56*, 1010.
(9) Sieck, L. W.; Lias, S. G.; Hellner, L.; Ausloos, P. *J. Res. Natl. Bur. Stand. A.* **1972**, *76A*, 115.

0002-7863/95/1517-7737$09.00/0

10^{-5} to 10^{-4} mol fraction of i-C_4H_8 added. The low concentrations were used in order to observe the variation of relative ion concentrations with reaction time, as several of the reactions proceed near the collision rate. The mixtures were prepared in a glass bulb heated to 150 °C, and C_6F_6, whose IP is higher than that of i-C_4H_8 by 0.67 eV,[21] was added in an excess of at least 10:1 to that of i-C_4H_8 to affect mild chemical ionization. We also observed that adding C_6F_6 increases the ion signal intensity because of its large ionization cross section and increases ion residence time due to the formation of negative ions by electron capture. The mixtures were ionized by a pulse of 1−2 keV electrons, and relative ion concentrations followed for 2−8 ms after the pulse.

For experiments with t-$C_4H_9^+$ and its products, the protonating reagent gas was CH_4, with trace CH_3Cl added for electron capture. Total source pressures ranged from 2 to 6 mbar, with 10^{-4} to 10^{-6} mol fraction of i-C_4H_8 in the kinetic experiments and 10^{-2} to 10^{-4} mol fraction of i-C_4H_8 in the equilibrium measurements. In these mixtures we observed series of ions corresponding to the formulas CH_3^+ (i-$C_4H_8)_n$, $C_2H_5^+$(i-$C_4H_8)_n$, and $C_3H_7^+$(i-$C_4H_8)_n$. We assume that the precursor fragment ions are formed by the exothermic protonation of i-C_4H_8 by CH_5^+ and $C_2H_5^+$.

Results and Discussion

1. The Overall Reaction Mechanism. The general reaction scheme following the generation of i-$C_4H_8^+$ is illustrated by the ion time profiles in Figure 1. The reactions following the selective formation of t-$C_4H_9^+$ in CH_4 carrier gas are shown in a figure available in the supporting information (Figure S1).

For the reaction system in Figure 1, the ionizing pulse first generates N_2^+ followed by N_4^+, which rapidly generates $C_6F_6^{\bullet+}$. These ions are not shown. This is followed by charge transfer to generate the i-$C_4H_8^+$ ion, which leads to the parallel reactions 1 and 2, which were reported previously.[5-8]

$$\text{i-}C_4H_8^{\bullet+} + \text{i-}C_4H_8 \rightarrow \text{t-}C_4H_9^+ + C_4H_7^{\bullet} \quad (1)$$

$$\rightarrow (\text{i-}C_4H_8^{\bullet+})\text{i-}C_4H_8 \quad (2)$$

The notation of (i-$C_4H_8^{\bullet+}$) i-C_4H_8 for the product of reaction 2 is not intended to indicate that this is a cluster ion; in fact, we shall present evidence that it is a covalent octene ion. It undergoes an H_2 transfer reaction 3 which is its major channel, as reported earlier.[5-7]

$$\text{i-}C_4H_8^{\bullet+}(\text{i-}C_4H_8) + \text{i-}C_4H_8 \rightarrow C_8H_{14}^{\bullet+} + C_4H_{10} \quad (3)$$

$$\rightarrow \text{i-}C_4H_8^{\bullet+}(\text{i-}C_4H_8)_2 \quad (4)$$

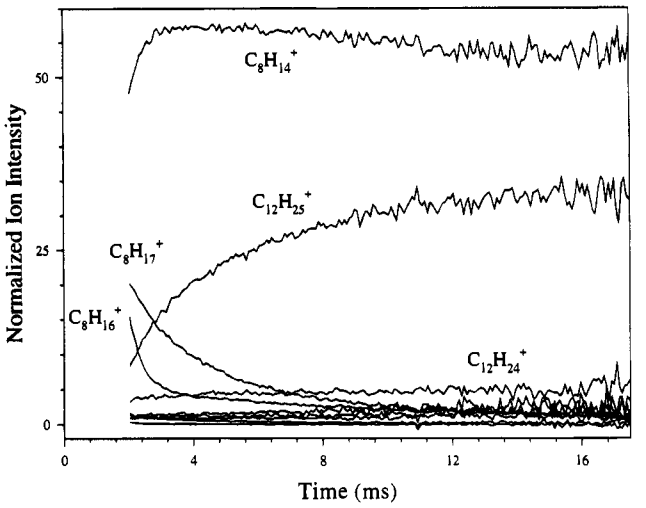

Figure 1. Normalized ion profiles ($100I_i/\sum I_i$) in a reaction mixture of 4.3 mbar of N_2 + 0.0056 mbar of C_6F_6 and 0.000052 mbar of i-C_4H_8 at 250 K. Unmarked ions less than 5% correspond to $C_4H_8^{\bullet+}$ and $C_4H_9^+$ (noise level), $C_{12}H_{22}^{\bullet+}$, $C_{16}H_{30}^{\bullet+}$, and $C_{16}H_{32}^{\bullet+}$.

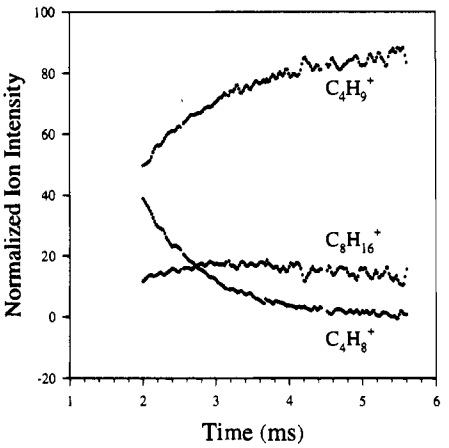

Figure 2. Parallel reactions of i-$C_4H_8^+$ with i-C_4H_8 to produce t-$C_4H_9^+$ and i-$C_4H_8^{\bullet+}$(i-C_4H_8). Normalized ion profiles in a reaction mixture of 6.1 mbar of N_2 + 0.0031 mbar of C_6F_6 and 0.000085 mbar of i-C_4H_8 at 501 K.

The product ion of reaction 3 does not undergo further addition reactions under our conditions, and this terminates the radical ion chain.

The carbonium ion t-$C_4H_9^+$ initiates a series of addition reactions of the general form

$$\text{t-}C_4H_9^+(\text{i-}C_4H_8)_{n-1} + \text{i-}C_4H_8 \rightarrow \text{t-}C_4H_9^+(\text{i-}C_4H_8)_n \quad (5)$$

We also observe that the product adducts undergo a series of H_2 transfer reactions, a novel process for carbonium ions, for example, reactions 6 and 7, as observed in the formation of the products in Figure 2.

$$\text{t-}C_4H_9^+(\text{i-}C_4H_8) + \text{i-}C_4H_8 \rightarrow C_8H_{15}^+ + \text{i-}C_4H_{10} \quad (6)$$

$$C_8H_{15}^+ + \text{i-}C_4H_8 \rightarrow C_8H_{13}^+ + \text{i-}C_4H_{10} \quad (7)$$

Similar H_2 transfer reactions are observed for the higher adducts, as observed in the consecutive formation of $C_{12}H_{23}^+$ and $C_{12}H_{21}^+$ from $C_{12}H_{25}^+$, and of $C_{16}H_{31}^+$ and $C_{16}H_{29}^+$ from $C_{16}H_{33}^+$. These reactions are shown in the ion time profiles available as supporting information (Figure S1). Fortunately, these reactions are slow and can be minimized at low concentrations, which allows quantitative studies on the association reactions.

(10) Mitchell, A. L.; Tedder, J. M. *J. Chem. Soc., Perkin Trans. 2* **1986**, 1197.
(11) (a) Meot-Ner (Mautner), M.; Field, F. H. *J. Am. Chem. Soc.* **1976**, *98*, 5576, (b) Koyano, I. *J. Chem. Phys.* **1966**, *45*, 706. Herman, J.; Herman, K.; Ausloos, P. *J. Chem. Phys.* **1970**, *52*, 28.
(12) Daly, G. M.; El-Shall, M. S. *J. Phys. Chem.* **1994**, *98*, 696.
(13) Solomon, J. J.; Meot-Ner (Mautner), M.; Field, F. H. *J. Am. Chem. Soc.* **1974**, *96*, 3727.
(14) Meot-Ner (Mautner), M.; Field, F. H. *J. Am. Chem. Soc.* **1975**, *97*, 2014.
(15) Meot-Ner (Mautner), M.; Field, F. H. *J. Chem. Phys.* **1976**, *64*, 277.
(16) Meot-Ner (Mautner), M.; Sieck, L. W. *J. Am. Chem. Soc.* **1991**, *113*, 4448.
(17) Meot-Ner (Mautner), M.; Field, F. H. *J. Am. Chem. Soc.* **1975**, *97*, 5339.
(18) Ceyer, S. T.; Tiedmann, P. W.; Ng, C. Y.; Mahan, B. H.; Lee, Y. T. *J. Chem. Phys.* **1979**, *70*, 2138.
(19) Ono, Y.; Linn, S. H.; Tzeng, W. B.; Ng, C. Y. *J. Chem. Phys.* **1984**, *80*, 1482.
(20) Stull, D. R.; Westrum, E. F.; Sinke, G. C. *The Chemical Thermodynamics of Organic Compounds*; John Wiley and Sons: New York, 1969.
(21) Lias, S. G.; Bartmess, J. E.; Liebman, J. F.; Holmes, J. L.; Levin, R. D.; Mallard, W. G. *J. Phys. Chem., Ref. Data* **1988**, *17*, Suppl. 1.

Table 1. Rate Coefficients[a] for the Branching Reaction i-$C_4H_8^{\bullet+}$ + i-C_4H_8 → t-$C_4H_9^+$ + C_4H_7 (k_1) and → i-$C_4H_8^{\bullet+}$(i-C_4H_8) (k_2) and for Charge Transfer Reactions of the Adduct, i-$C_4H_8^+$(i-C_4H_8) + B → $B^{\bullet+}$ + C_8H_{16} (k_8)

T (K)	k_1[a]	k_2[a]	$k_1 + k_2$[a]
250	0.4	1.4	1.8
303	0.6	1.2	1.8
401	0.7	0.8	1.5
437	0.4	0.6	1.0
497	0.5	0.2	0.72
565	0.6	0	0.60
625	0.5	0	0.46

bracketing reactions	T (K)	k_8
$C_6H_5CH_3$	391	<0.01
C_6H_5-n-C_4H_9	391	<0.01
1,3,5-$C_6H_3(CH_3)$	391	1.6

[a] Units of 10^{-9} cm^3 s^{-1}. k_1 and k_2 are calculated from the measured overall rate coefficient and product distributions, see Figures 4 and 5. Experimental conditions are given in the caption of Figure 4. Uncertainty is estimated from four sets of 3−5 replicate measurements by multiplying the standard deviation of ln k by a coverage factor of 2 for a confidence interval of 0.95. This leads to an uncertainty multiplier of 1.6, so that the reported values are precise within a factor of 1.6 with a confidence level of 95%.

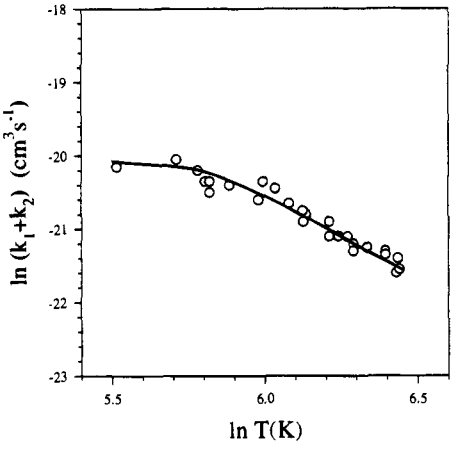

Figure 3. Temperature dependence of rate coefficient of the reaction of i-$C_4H_8^{\bullet+}$ with i-C_4H_8 ($\ln(k_1 + k_2)$) (cm^3 s^{-1}) vs ln$T$). Measurements in reaction mixtures of N_2 + 2.6 × 10^{-4} mol fraction of C_6F_6 at a constant density of 7.8 mol cm^{-3}, with 7.5 × 10^{-6}, 8.0 × 10^{-6}, and 1.4 × 10^{-5} mol fraction of i-C_4H_8.

The following sections address specific aspects of the key reactions.

2. Reactions of the i-$C_4H_8^{\bullet+}$ Ion. Evidence for Distinct Direct and Complex-Forming Collisions. The Structure of i-$C_4H_8^{\bullet+}$(i-C_4H_8). Reactions 1 and 2 can be studied quantitatively at low concentrations where the subsequent reactions are slow. An example is shown in Figure 2. The reaction into both channels is irreversible, and from the decay of the i-$C_4H_8^{\bullet+}$ ion we can derive the overall forward rate coefficient $k_1 + k_2$. Furthermore, from the product distribution we obtain k_1/k_2, and from these data, the individual rate coefficients k_1 and k_2.

The results are shown in Table 1 and in Figures 3 and 4. The overall rate coefficient is near the collision rate at low temperatures, but decreases at higher temperatures, due to the decreasing rate coefficient of the association reaction, which becomes negligible at high temperatures. On the other hand, the rate coefficient for proton transfer reaction remains approximately constant over the entire temperature range. The observed behavior can be explained by the two reactions proceeding through two distinct channels. The proton transfer reaction apparently proceeds by a direct mechanism which is independent of temperature. The other channel leads to a

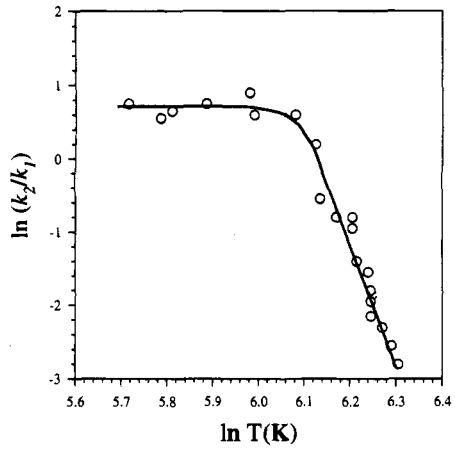

Figure 4. Temperature dependence of the product distribution of i-$C_4H_8^{\bullet+}$ + i-C_4H_8 → t-$C_4H_9^+$ + C_4H_7 and i-$C_4H_8^{\bullet+}$(i-C_4H_8), expressed as ln(k_2/k_1). Reaction conditions are the same as in Figure 4.

complex which either becomes stabilized or back-dissociates to reactants at increasing rates with increasing temperature. A similar mechanism was proposed for the competitive proton transfer or association of carbonium ions with amines.[17]

Because of the limited pressure range, no systematic studies were conducted on the pressure dependence of the product ratio. Qualitatively, we found that the adduct/proton transfer ratio decreases with increasing total ion source pressure. This is contrary to expectation if the excited adduct is collisionally stabilized. In fact, collisional stabilization is suggested by the fact that the association channel is not observed under low-pressure (<10^{-3} mbar) conditions.[7,8]

We observe in Figure 2 that the association reaction is irreversible. This shows that the equilibrium ion ratio of I(i-$C_4H_8^{\bullet+}$(i-C_4H_8))/I(i-C_4H_8) is >10 under the conditions described in the caption of Figure 2. From this limiting ion ratio we calculate $\Delta G°_2(501)$ < −78 kJ/mol (−19 kcal/mol). Assuming $\Delta S°$ = −109 ± 18 J/(mol K) (−26 cal/(mol K)) for a non-covalent clustering reaction, we obtain $\Delta H°_2$ < −132 ± 9 kJ/mol (−32 ± 2 kcal/mol); a more negative entropy change for covalent association would yield an even larger $-\Delta H°$. In comparison, the binding energy of the ethene dimer ion $C_2H_4^{\bullet+}$-(C_2H_4) is <80 kJ/mol (19 kcal/mol).[18,19] Therefore the lower limit of the binding energy is significantly larger than may be expected for a π complex cluster ion.

We obtained further information on the nature of the product by bracketing the ionization potential using charge transfer reactions 8.

$$\text{i-}C_4H_8^{\bullet+}\text{(i-}C_4H_8\text{)} + B \rightarrow B^{\bullet+} + C_8H_{16} \qquad (8)$$

The measurements were conducted at 391 K, at a source pressure of 5.9 mbar, with 1.8 × 10^{-4} mol fraction of i-C_4H_8 and 2 × 10^{-5} to 4 × 10^{-6} mol fraction of alkylbenzene reactant. Under these conditions the (i-$C_4H_8^{\bullet+}$)i-C_4H_8 adduct forms rapidly and irreversibly, and its reactivity with the aromatics which are added at low concentrations can be observed. We found that with $C_6H_5CH_3$ (IP = 8.82 eV) and C_6H_5-n-C_4H_9 (IP = 8.68 eV) the adduct was unreactive, but it reacted rapidly with 1,3,5-$C_6H_3(CH_3)_3$ (IP = 8.41 eV), as shown in Table 1. This brackets the IP of i-$C_4H_8^{\bullet+}$(i-C_4H_8) as 8.55 ± 0.15 eV. This can be combined with an estimated $\Delta H°_f$ for branched C_8H_{16} alkenes of −108 ± 2 kJ/mol (−25.5 ± 0.5 kcal/mol)[20] to obtain the $\Delta H°_f(300)$ of the adduct (i-$C_4H_8^{\bullet+}$) i-C_4H_8 as 718 ± 17 kJ/mol (172 ± 4 kcal/mol).

In comparison, octenes with two or more CH_3 substituents on an olefinic carbon have lower IPs (8.2 ± 0.1 eV)[21] and the

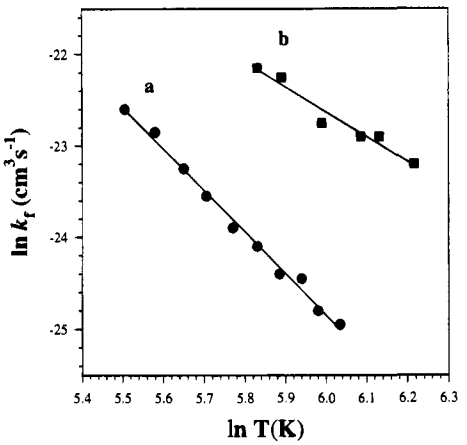

Figure 5. Temperature dependence of the rate coefficients for H_2 transfer reactions: (a) i-$C_4H_8^{\bullet+}$(i-C_4H_8) + i-C_4H_8, in a reaction mixture of N_2 + 1.1 × 10^{-3} mol fraction of C_6F_6 and 2.4 × 10^{-5} mol fraction of i-C_4H_8, at a constant total density of 6.5 × 10^{16} cm^{-3}; (b) $(CH_3)_2$-$CCH(CH_2)_3CH_3^{\bullet+}$ + $(CH_3)_2CCH(CH_2)_3CH_3$ in a reaction mixture of N_2 + 5.0 × 10^{-4} mol fraction of C_6F_6 and 1.8 × 10^{-5} mol fraction of $(CH_3)_2CCH(CH_2)_3CH_3$ at a constant total density of 6.7 × 10^{16} cm^{-3}.

ions have lower $\Delta H°_f$ values. For a compound with one CH_3 substituent on an olefinic carbon, we bracketed the IP of $(CH_3)_2$-$CCHCH_2CH_2CH_2CH_3$ between that of 1,3,5-$C_6H_5(CH_3)_3$ (IP = 8.41 eV) and $C_6H_5OCH_3$ (IP = 8.21 eV),[21] which yields IP($(CH_3)_2CCHCH_2CH_2CH_2CH_3$) as 8.3 ± 0.1 eV. We also observed directly that the adduct (i-$C_4D_8^+$)i-C_4D_8 reacted rapidly through charge transfer with $(CH_3)_2CCHCH_2CH_2CH_2CH_3$, which is also consistent with the adduct having a higher IP. Therefore any structure with a CH_3 substituent on an olefinic carbon is not consistent with the bracketed IP.

For the $C_8H_{16}^+$ olefin ions whose $\Delta H°$ is available,[21] the result for the adduct is closest to the $\Delta H°_f$ of $(C_2H_5)_2CCHCH_2CH_3^{\bullet+}$, but this isomer would require substantial skeletal rearrangement. A possible isomer may be $(CH_3)_2CHCHCHCH(CH_3)_2^{\bullet+}$, with $\Delta H°_f$ of 745 kJ/mol (178 kcal/mol) for the *E* conformer and 749 kJ/mol (179 kcal/mol) for the *Z* conformer.[21] This could be produced by tail-to-tail addition of i-$C_4H_8^+$ to i-C_4H_8 which should be favored sterically and also because it would produce $(CH_3)_2C^+CH_2CH_2C^{\bullet}(CH_3)_2$ in which both the ionic and radical sites are stabilized on tertiary carbons. The condensation can be followed by two hydrogen shifts to yield $(CH_3)_2CHCHCHCH$-$(CH_3)_2^{\bullet+}$. It would be puzzling, however, that the same reaction with only one hydrogen shift would place a double bond on a CH_3-substituted carbon, giving $(CH_3)_2CCHCH_2CH(CH_3)_2^{\bullet+}$ which should be more stable.

The reactivity of the ion, as discussed in the next section, is also consistent with a covalent adduct.

3. Kinetics of H_2 Transfer Reactions. The occurrence of H_2 transfer reactions between alkene radical ions and alkanes was reported in early radiolytic and mass spectrometric experiments.[5-7] In the present work we report H_2 transfer reactions involving new types of reactants, namely alkene radical ions or even-electron carbonium ions with alkenes. Such reactions are evident in Figure 1 and Figure S1 in the supporting information involving the i-$C_4H_8^{\bullet+}$(i-C_4H_8)$_n$ and t-$C_4H_9^+$(i-C_4H_8)$_n$ adducts.

For a quantitative study, we used low-temperature and low-concentration conditions, for example, in a reaction mixture of 8.4 mbar of N_2, 0.0024 mbar of C_6F_6, and 0.000063 mbar of i-C_4H_8 at 297 K, or the conditions described in the caption of Figure 5. The measured rate coefficient for reaction 3 was constant when the concentration was varied by a factor of 4 and the pressure by a factor of 2. The rate coefficients are given in Table 2, and the temperature dependence is shown in Figure 5.

Table 2. Rate Coefficients of H_2 Transfer Reactions

	T	k^a	$aT^{n\,b}$
i-$C_4H_8^{\bullet+}$(i-C_4H_8) + i-C_4H_8 →	421	0.015	$2.2T^{-4.3}$
$C_8H_{14}^{\bullet+}$ + i-C_4H_{10}	381	0.023	
	301	0.058	
	247	0.15	
$(CH_3)_2CCH(CH_2)_3CH_3^+$ +	501	0.079	$0.0023T^{-2.8}$
$(CH_3)_2CCH(CH_2)_3CH_3$ →	461	0.11	
$C_8H_{14}^+$ + C_8H_{18}	401	0.14	
	341	0.23	

[a] Units of 10^{-9} cm^3 s^{-1}. For uncertainty estimates see footnote *a*, Table 1. [b] Equation for the rate coefficient in the functional form $k = aT^n$.

To ascertain whether an H_2 transfer reaction is possible for an octene radical ion, we examined reaction 9 under the conditions described in the preceding paragraph.

$$(CH_3)_2CCH(CH_2)_3CH_3^{\bullet+} + (CH_3)_2CCH(CH_2)_3CH_3 \rightarrow C_8H_{14}^{\bullet+} + C_8H_{18} \quad (9)$$

We observe that the reaction indeed occurs, with rate coefficients and temperature coefficients in the same range as those for reaction 3, as shown in Table 2 and Figure 5. This further supports reaction 3, although in reaction 9 the same products would also result from an H_2^- transfer reaction.

The slow rates and negative temperature coefficients of the H_2 transfer reactions may be caused by entropy barriers due to the hindrance of rotors during the approach to a tight complex, similar to those in H^- transfer reactions.[13-15,22,23] A central barrier with a low density of states may also contribute. It is also possible that H_2 transfer reactions consist of two stages involving proton transfer, followed by slower, rate-controlling hydride transfer. The second step would explain the kinetic similarity to hydride transfer reactions.

In contrast to reactions 3 and 9, the i-$C_4H_9^+$ ion is not known to undergo H_2 transfer with alkenes. The kinetic similarity of reaction 3 to reaction 9 which involves a known octene ion is also consistent with a covalent structure for (i-$C_4H_8^+$)i-C_4H_8 also being a covalently bonded octene ion. A further useful experiment would be to examine whether known octene ions transfer H_2 to i-C_4H_8.

Since the H_2 transfer reactions are fast at low temperatures, and since the product $C_8H_{14}^{\bullet+}$ was not observed to add further i-C_4H_8 significantly, the H_2 transfer reaction can terminate the radical polymerization branch. Further, at high temperatures the formation of the $C_4H_8^{\bullet+}$(i-C_4H_8) adduct is slow. Combined, these observations may explain why i-C_4H_8 does not undergo radical cation polymerization.

We also observed H_2 transfer reactions in the carbonium ion branch, from the t-$C_4H_9^+$(i-C_4H_8)$_n$ ion to i-C_4H_8 as noted above for reactions 6 and 7. We identify these as bimolecular H_2 transfer reactions rather than unimolecular pyrolytic H_2 loss because their rates increased with increasing i-C_4H_8 concentration. From qualitative observations, these are also slow reactions several orders of magnitude below the collision rate.

4. Entropy Barriers to Polymerization: Consecutive Condensation Reactions Initiated by t-$C_4H_9^+$. The carbonium ion t-$C_4H_9^+$ is generated in reaction 1. Its chemistry can be best observed using a protonating reagent gas such as CH_4, where the radical ions are absent. The ions observed under these

(22) Sunner, J. A.; Hirao, K.; Kebarle, P. *J. Phys. Chem.* **1989**, *93*, 4010.
(23) Meot-Ner (Mautner), M.; Smith, S. C. *J. Am. Chem. Soc.* **1991**, *113*, 862.

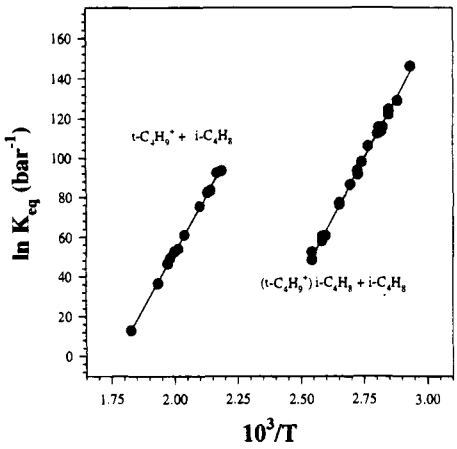

Figure 6. Van't Hoff plots for the association reactions shown. Points for the t-$C_4H_9^+$ + i-C_4H_8 equilibrium were obtained in mixtures of 1.6 × 10^{-4} or 5.8 × 10^{-2} mol fraction of i-C_4H_8 in CH_4, at pressures between 4.5 and 5.9 mbar. Points in the t-$C_4H_9^+$(i-C_4H_8) + i-C_4H_8 plot were obtained at i-C_4H_8 concentrations of 4.2 × 10^{-4}, 1.7 × 10^{-2}, and 3.7 × 10^{-2} mol fractions in CH_4 at pressures between 3.5 and 6.4 mbar.

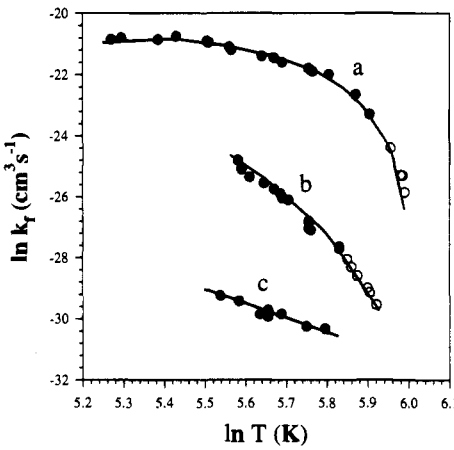

Figure 7. Temperature dependence of the consecutive association reactions of t-$C_4H_9^+$ with i-C_4H_8. The points indicated by solid circles were achieved under irreversible conditions, while those indicated by open circles were achieved under reversible conditions: (a) t-$C_4H_9^+$ + i-C_4H_8; (b) t-$C_4H_9^+$(i-C_4H_8) + i-C_4H_8; (c) t-$C_4H_9^+$(i-C_4H_8)$_2$ + i-C_4H_8.

conditions are shown in Figure S1 in supporting information. For quantitative studies, we used low concentrations where the H_2 transfer reactions are negligible.

The first two condensation steps were observed to be reversible. To verify the equilibrium we performed measurements at reactant concentrations varying over an order of magnitude for the first and second steps, as described in the caption of Figure 6. We observed that the measured equilibrium constant was not affected. We also observed that the rate coefficients for the association reactions measured at various concentrations were consistent. Furthermore, the rate coefficients measured from approach to equilibrium using reversible kinetics were consistent with extrapolation from rate coefficients measured at lower temperatures under irreversible kinetics, as shown in Figure 7.

The fact that the association reactions are reversible under some conditions does not necessarily suggest that the products are non-covalently bonded clusters. The reverse process to condensation is pyrolysis, and such reactions were reported for C_6 and higher carbonium ions.[24] In fact, the thermochemistry of the first step [$\Delta H°$ = −95.8 kJ/mol (−22.9 kcal/mol), $\Delta S°$ = −136.8 J/(mol K) (−32.7 cal/(mol K))], as shown in Table 3, is consistent with the formation of a branched C_8 carbonium ion. Estimates can be made using the $\Delta H°_f$i-C_4H_8 and t-$C_4H_9^+$, the estimated $\Delta H°_f$, and PA of a branched octene (estimating the PA to be about 4 kcal/mol above i-C_4H_8).[20,21] This yields an estimated $\Delta H°_5$ (n = 1) of −75 to −92 kJ/mol (−18 to −22 kcal/mol), in good agreement with the observed value. For $\Delta S°$, we can use $\Delta S°$ for i-C_4H_{10} + i-C_4H_8 → branched C_8H_{18} which is −146 to −168 J/(mol K) (−35 to −40 cal/(mol K)),[20] again in reasonable agreement with the results.

Table 3. Thermochemistry and Kinetics of Association Reactions

	T	k^a	$-\Delta H°$ [b]	$-\Delta S°$ [b]
t-$C_4H_9^+$ + i-C_4H_8	401	0.0060	95.8(±4)	136.8(±7)
	367	0.078		
	320	0.29		
	289	0.47		
	245	0.78		
	228	0.96		
(i-$C_4H_9^+$)i-C_4H_8 + i-C_4H_8	371	0.00015	101.3(±6)	203.7(±8)
	341	0.00095		
	297	0.0049		
	265	0.017		
(t-$C_4H_9^+$)(i-C_4H_8)$_2$ + i-C_4H_8	313	0.000072		
	295	0.00011		
	265	0.00017		
	253	0.00020		
(t-$C_4H_9^+$)(i-C_4H_8)$_3$ + i-C_4H_8	285	0.000054		

[a] Units of 10^{-9} cm^3 s^{-1}. Uncertainty in PHPMS rate constant measurements is usually ±30%. [b] $\Delta H°$ in kJ/mol, $\Delta S°$ in J/(mol K). Uncertainty from standard deviations of the slopes and intercepts of van't Hoff plots of n points, multiplied by Student's t factors for confidence levels of 95% for n − 2 degrees of freedom.

For steric reasons, the first association step probably involves the attack of the t-$C_4H_9^+$ ion on the primary methylene group of $(CH_3)_2CCH_2$ to yield the sterically crowded $(CH_3)_3CCH_2C(CH_3)_2^+$ ion. The second association step requires further attack of this ion on $(CH_3)_2CCH_2$ leading to a thermochemistry [$\Delta H°$ = −101.3 kJ/mol (−24.2 kcal/mol), $\Delta S°$ = −203.7 J/(mol K) (−48.7 cal/(mol K))] with a $\Delta S°$ value that is more negative by 67 J/(mol K) (16 cal/(mol K)) than for a typical condensation reaction such as the first condensation step. The thermochemistry of alkanes shows that branched hydrocarbons with sterically interfering methyl groups may have entropies lower by 42 to 62 J/(mol K) (10 to 15 cal/(mol K)) than less crowded isomers.[20] Therefore the observed value is reasonable for a branched and sterically crowded product ion. We note that the alternative low-entropy product, a saturated cyclic protonated alkane ion, is unlikely, and in fact it would probably will be reactive in this system, transferring the proton to the i-C_4H_8 reactant in the reaction mixture.

The kinetic results are also consistent with a hindered product in this step, as will be discussed presently.

5. Kinetics of the Consecutive Condensation Reactions of the t-$C_4H_9^+$ Ion. We obtained kinetic data from approach to equilibrium where the reactions were reversible and from irreversible kinetics at lower temperatures. For the first step we performed a pressure study at 337 K, and for the second step at 320 K, both for total source pressures between 2.4 and 6.4 mbar. Both showed that the reaction is pseudo second order at these, and therefore also at lower, temperatures. The sharp drop-off of the rate coefficient for the first step above 360 K (Figure 7) may be due to transition to third-order kinetics, but the slow rates at these temperatures do not allow a meaningful pressure study. Below 220 K the rate coefficient levels off near the collision rate. The measurements in this range may be affected by partial condensation of i-C_4H_8 in the ion source.

For the second step, the temperature coefficient is strongly negative over the entire range, with a temperature coefficient of T^{-12} to T^{-16}. We also confirmed the kinetics in a measure-

(24) Meot-Ner (Mautner), M.; Field, F. H. *J. Phys. Chem.* **1976**, *80*, 2865.

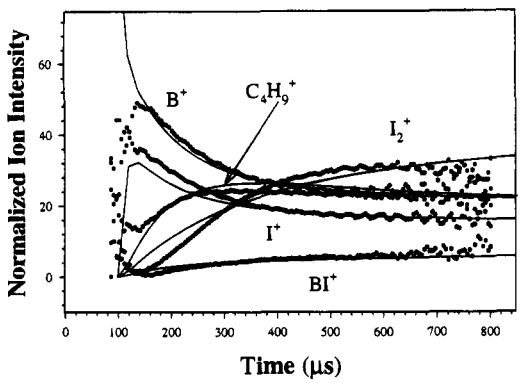

Figure 8. Ion time profiles in a reaction mixture of 1.7×10^{-3} mol fraction of i-C_4H_8 and 1.1×10^{-2} mol fraction of C_6H_6 at 0.18 mbar N_2 and 315 K. I = i-C_4H_8; B = C_6H_6.

ment using i-C_4D_8. Although analogy with bimolecular reactions is not direct, large negative temperature coefficients in reactions of bulky carbonium ions and hindered pyridines have been reported.[13-16,22,23] Slow rates and large negative temperature coefficients resulted from the freezing of rotors in the reaction complex. Therefore the large negative temperature dependence is consistent with the formation of a hindered branched carbonium ion, as the thermochemistry also suggests.

The third condensation step is still slower, but with a smaller temperature coefficient. This reaction could be observed only at low temperatures where no equilibrium was observed. We could measure the fourth step only at one temperature, at which it was slower yet than the third step.

6. The Benzene–Isobutene System. In the following paper we photoionize mixed benzene–isobutene clusters. For comparison, we examined here the analogous gas-phase system. We used a high-pressure ion source with a window that admits laser photons into a mixture containing C_6H_6 and i-C_4H_8 in N_2 carrier gas. We applied two-photon resonance ionization using the $A_{1g} \rightarrow B_{2u}6_0^1$ benzene transition at 258.9 nm which exhibits an isolated molecule lifetime of 100 ns. Details of the apparatus will be reported elsewhere.[25]

We observed that under the experimental conditions used, no benzene fragments were generated in the two-photon fluence regime. We also observed no direct photoionization of isobutene in the absence of C_6H_6 in the reaction mixture. Therefore the observed isobutene ions must be generated by charge transfer from $C_6H_6^+$ ions.

The time profiles of the observed ions and the results of a kinetic simulation are shown in Figure 8. The simulations suggest that the $C_4H_9^+$ and $C_8H_{16}^{\bullet+}$ ions are produced by the parallel reactions 1 and 2. The overall reaction is summarized in reactions 1, 2, 10, and 11.

$$C_6H_6^{\bullet+} + \text{i-}C_4H_8 \rightarrow \text{i-}C_4H_8^{\bullet+}(C_6H_6) \rightarrow \text{i-}C_4H_8^{\bullet+} + C_6H_6 \quad (10)$$

$$\text{i-}C_4H_8^{\bullet+} + \text{i-}C_4H_8 \rightarrow \text{t-}C_4H_9^+ + C_4H_7 \quad (1)$$

$$\rightarrow \text{i-}C_4H_8^{\bullet+}(\text{i-}C_4H_8) \quad (2)$$

$$\text{i-}C_4H_8^{\bullet+}(C_6H_6) + \text{i-}C_4H_8 \rightarrow \text{i-}C_4H_8^{\bullet+}(\text{i-}C_4H_8) + C_6H_6 \quad (11)$$

The kinetic simulations were performed using the ACUCHEM program obtained from NIST.[26] The rate coefficients used for reactions 1 and 2 were obtained from Table 1. The simulations showed reasonable agreement with the experimental time profiles in Figure 8. It should be noted that including the exchange reaction 11 was necessary in order to best simulate the time profiles, although visually, the adduct i-$C_4H_8^{\bullet+}(C_6H_6)$ does not show a decay suggestive of this reaction.

The adduct i-$C_4H_8^{\bullet+}(C_6H_6)$ is of interest since the ionization energy difference between the components is only 0.1 eV. Therefore, according to previous observations on aromatic charge transfer complexes, the complex may be stabilized by charge transfer resonance contributions.[27,28] From the data in Figure 8, the equilibrium ion ratio of $(C_6H_6(\text{i-}C_4H_8))^{\bullet+}/C_6H_6^{\bullet+}$ is >0.2, therefore for the association reaction, $\Delta G°_{300} < -18.4$ kJ/mol (−4.4 kcal/mol). Assuming a $\Delta S°$ of -109 ± 18 kJ/mol (-26 ± 4 cal/(mol K)), we obtain for the binding energy of the complex $\Delta H° < -53 \pm 6$ kJ/mol (-13 ± 2 kcal/mol).

At higher isobutene concentrations we observed reaction 3 leading to the formation of $C_8H_{14}^{\bullet+}$ which did not show further reactivity. We also observed the formation of higher t-$C_4H_9^+$-$(\text{i-}C_4H_8)_n$ adducts according to reaction 5. The behavior of i-$C_4H_8^{\bullet+}$ generated through the nearly thermoneutral charge transfer from $C_6H_6^{\bullet+}$ was therefore similar to that generated by more exothermic charge transfer from $C_6F_6^{\bullet+}$ in the preceding experiments. The gas-phase reactions in this system will be compared to observations in C_6H_6–i-C_4H_8 mixed clusters in the following paper.

Conclusions

Although cationic polymerization is important in technology and in nature, only limited kinetic information is available for a few systems, and this consists mostly of rate coefficients at room temperature. In the present study, equilibrium temperature studies, or limits on equilibrium constants at elevated temperatures, yielded thermochemical data with structural implications on the polymerization intermediates. Kinetic studies show new reactions, such as H_2 transfer from carbonium ions. The results reveal negative temperature coefficients for most of the reactions of interest. This shows that the slow rates of H_2 transfer reactions are due mainly to entropic effects such as steric hindrance.

The H_2 transfer reactions yield unreactive polyunsaturated olefin radical ions, and therefore may be effective polymerization chain terminators. Such reactions seem to be ubiquitous in hydrocarbon systems in the presence of alkenes, as they occur both in alkane and alkene radical ions and in carbonium ions. The negative temperature coefficient also suggests that H_2 transfer reactions will be fast under interstellar conditions. Because of their apparent ubiquity, further studies on H_2 transfer reactions would be of interest.

Of particular interest is the observed entropy barrier to condensation in the carbonium ion system. This may have practical implications. Entropy barriers can make the negative temperature coefficients of association reactions even steeper than usual. If similar factors are responsible for the slow rates of high polymerization steps in alkenes, then the rates may increase sharply at the low-temperature interstellar conditions, where such reactions may approach the collision rate. On the other hand, at flame temperatures such reactions may become negligibly slow. This also suggests that such reactions may be accelerated for industrial uses by applying low temperatures.

(25) Daly, G. M.; Meot-Ner (Mautner), M.; Pithawalla, Y.; MacPherson, J.; El-Shall, M. S. *J. Chem. Phys.* Submitted for publication.

(26) ACUCHEM Version 1.4, copyright National Institute of Standards and Technology, November 7, 1986.

(27) Meot-Ner (Mautner), M.; Hamlet, P.; Hunter, E. P.; Field, F. H. *J. Am. Chem. Soc.* **1978**, *100*, 5466.

(28) Meot-Ner (Mautner), M.; El-Shall, M. S. *J. Am. Chem. Soc.* **1986**, *108*, 4386.

The present work is the first study of an ionic polymerization system on the level of detail that is allowed by variable-temperature measurements. The results allow insights about the controlling factors in a gas-phase polymerization system. In the following paper we shall examine whether these effects also apply in the cluster environment.

Acknowledgment. This work was supported in part (L.W.S.) by a grant from the Office of Basic Energy Sciences, US Department of Energy and by the National Science Foundation (Grant No. CHE9311643 to M.S.E.). M.S.E. also acknowledges the donors of the Petroleum Research Fund (2764-AC6), administered by the American Chemical Society, the Thomas F. and Kate MIller Jeffress Memorial trust (J-302), and the Exxon Education Foundation for partial support of this research.

Supporting Information Available: Two figures of ion time profiles (3 pages). This material is contained in many libraries on microfiche, immediately follows this article in the microfilm version of the journal, can be ordered from the ACS, and can be downloaded from the Internet; see any current masthead page for ordering information and Internet access instructions.

JA950855P